AMERICAN JOURNAL OF PHARMTECH RESEARCH
Journal home page: http://www.ajptr.com/

Preparation, Characterization and Surface Modification of Nevirapine Nanoparticles

Bhagyashree R. Dalvi[1], Rupesh U. Shelke[1], Ejaz A. Siddiqui[2], Asad S. Syed[2], Mariam S. Degani[1], Padma V. Devarajan[1]*,Absar Ahmad[2]
1. Department of Pharmaceutical Sciences and Technology, Institute of Chemical Technology, N.P. Marg, Matunga (E), Mumbai, Maharashtra, India
2. Biochemical Sciences Division, CSIR-National Chemical Laboratory, Pune, India.

ABSTRACT

HIV/AIDS is an intracellular infection of the macrophages and play an important role in dissemination of the infection across the body. Nevirapine although remains a drug of choice for the treatment; the life threatening hepatotoxicity limits its clinical application. Present study reports preparation, characterization and surface modification of nevirapine nanoparticles. The anti-HIV potential of gold nanoparticles prompted us to prepare nevirapine loaded gold nanoparticles using a biodegradable in house polymer polyethylene sebacate. Core shell nevirapine nanoparticles comprising gold in the core and nevirapine loaded polyethylene sebacate as shell (average particle size ~ 250nm) were successfully prepared using double emulsion solvent evaporation method followed by surface modification with macrophage mannose receptor targeting ligand Concanavalin A by simple incubation. Concanavalin A was selected as a targeting ligand as the molecular docking studies of Concanavalin A with excipients suggested possible interactions. Concanavalin A anchoring was confirmed by spectrofluoremetrically, FTIR and zeta potential analysis. UV analysis of nevirapine nanoparticles revealed shell formation and NVP loading. SEM-EDAX analysis indicated presence of Au in the spherical nanoparticles while TEM confirmed formation of core shell nanoparticles with smooth surface. DSC and XRD analysis demonstrated amorphization of NVP in nanoparticles. Residual solvent analysis complied ICH standards. Nanoparticles with and without CON exhibited sustained release till 24 h in phosphate buffer pH 7.4 and good stability for 1 year as per ICH guidelines.

Keywords: HIV/AIDS, macrophages, nevirapine, gold nanoparticles, concanavalin A, spectrofluoremetry.

*Corresponding Author Email: pvdevarajan@gmail.com
Received 30 July 2015, Accepted 05 August 2015

Please cite this article as: Devarajan PV.*et al*., Preparation, Characterization and Surface Modification of Nevirapine Nanoparticles. American Journal of PharmTech Research 2015.

INTRODUCTION

HIV/AIDS is an intracellular infection of macrophages that is localized mainly in the reticuloendothelial system (RES) organs namely liver, spleen, lung, lymph node and lymphocytes[1, 2]. Macrophages provide a safe haven for the HIV and are also responsible for dissemination of the infection particularly to remote locations like the brain and bone marrow[3-5]. Nevirapine (NVP) is one of the key components of highly active antiretroviral therapy used for the treatment as well as for prophylactic purpose in the management of HIV-1 infections. Despite of high and proven therapeutic advantage the life threatening hepatotoxicity limits its use in the situations where benefit to the patient exceeds risk[6]. Nanoparticulate carriers holds promise in the eradication of the HIV infection, because it could provide targeted and sustained anti-retroviral drug delivery with notably high drug concentrations in the HIV reservoirs and amelioration of toxicity[7]. Targeted delivery of nevirapine to macrophages through receptor mediated endocytosis represents an attractive approach for improved efficacy and decreased toxicity. Macrophages possess various receptors on its surface such as mannose, folate, transferrin galactosyl, scavenger and Fc receptors[8]. Mannose receptors are present on the surface of monocyte/macrophages, kupffer cells in liver, alveolar macrophages, astrocytes in brain, dendritic cells etc. Macrophage targeting through mannose receptors proved successful for targeting stavudine[2], indinavir[9], zidovudine[10], didanosine[11,12], lamivudine[13], efavirenz [14,15] to macrophage rich tissues liver, spleen, lung, brain and lymph nodes. Mannosylated liposomes exhibited 2-4 fold higher drug levels than unmodified liposomes in kupffer cells & peritoneal macrophages[16]. Mannobiose monoarachidic acid esters surface modified liposomes demonstrated rapid and enhanced uptake in liver and spleen[17]. Decreased hepatotoxicity of anti-tubercular drugs was revealed by wheat germ agglutinin modified poly (lactide-co-glycolide) nanoparticles through selective kupffer cell targeting[18]. Concanavalin (CON) A is a lectin having high affinity for mannosylated residues[19]. Concanavalin A proven effective in preventing fusion of HIV infected cells with CD4 cells presumably through interactions with HIV gp120 envelop molecule[20]. Lectin (mannose) receptors are present on the surface of macrophages. Drug loaded nanoparticles conjugated with CON would efficiently target these nanoparticles to macrophages. Polyethylene sebacate (PES) a biodegradable polymer developed in our lab offers some unique advantages over other polymers which includes ease of synthesis, good hydrolytic stability and low cost and no toxicity[21]. Herein we discuss the design of polyethylene sebacate-nevirapine-gold nanoparticles and further surface functionalization with concanavalin by simple adsorption technique. The aim of the study was to exploit physical

adsorption as a simple method for the design of concanavalin loaded nevirapine nanoparticles. The objective of the study was to confirm the concanavalin loading and feasibility of the adsorption technique for loading concanavalin.

MATERIALS AND METHOD

Materials

Nevirapine (Macleods Pvt. Ltd., Mumbai, India), Polyethylene sebacate (synthesized in our lab, molecular weight = 11300) and HPLC grade acetonitrile (Azeocryst Organics Pvt. Ltd., Mumbai, India) were obtained as gift samples. Presynthesized AuNPs were obtained from Dr. Absar Ahmad's Lab (National Chemical Laboratory, Pune), dioctyl sodium sulfosuccinate (AOT), dichloromethane (DCM), sodium dihydrogen orthophosphate, Tween 80 were purchased from S. D. Fine-Chem limited (Mumbai, India). Concanavalin A and phosphate buffer saline (PBS) were purchased from Himedia laboratories Pvt. Ltd.

Preparation of polyethylene sebacate-nevirapine-gold nanoparticles (PES-NVP-AuNPs)

The double emulsion solvent evaporation (DESE) water in oil in water, (W/O/W) method was employed to prepare PES-NVP-AuNPs. A predetermined quantity of PES, AOT and NVP was dissolved in 10 mL DCM (organic phase). An aqueous gold nanoparticles dispersion (100 µL) was added drop wise to the organic phase and vortexed to form a primary W/O emulsion, which was further dispersed in 20 mL of an aqueous phase comprising 2 % w/v tween 80 solution under probe sonication (DP120, Dakshin, Mumbai, India) for 10 min (10sec on/10sec off cycle, 150 V) to form a W/O/W double emulsion. The evaporation of DCM from the emulsion was achieved under magnetic stirring for 2-3 h at 30 ± 5^{o}C. The resulting nanoparticulate dispersion was centrifuged (Eltek 4100 D Research Centrifuge) at 20,000 rpm for 20 min, the supernatant collected and analyzed by UV spectrophotometer (UV-1650 PC UV-Visible spectrophotometer, Shimadzu) for NVP to determine entrapment efficiency. The isolated pellet was redispersed in 8 mL deionized water and sonicated in a bath sonicator for 10 min. Following addition of trehalose as cryoprotectant, the nanodispersion was freeze dried. The effect of AOT concentration (0.15, 0.2 and 0.25% w/v) on the particle size and % entrapment efficiency (% EE) was evaluated.

Molecular docking study of concanavalin A with nevirapine and polyethylene sebacate

The Glide molecular docking protocol implemented within the Maestro (Schrödinger, LLC, New York, NY, 2008) was used to understand the interactions between CON and PES/NVP. The crystal structure of CON retrieved from the protein data bank with PDB code 2UU8 (Acta Crystallogr.,Sect.D **63:** 906) was selected for the docking experiment. Water molecules were

deleted in the protein preparation step. Site map analysis was performed to find out possible active sites on CON. Grids were generated using sites defined by sitemap analysis. Ligand structures (PES oligomer and NVP) were constructed using build option within Maestro. With the help of Ligprep facility, low-energy 3D conformation was generated for each of the ligand by energy minimization with a dielectric constant of 1.0 and docked into the active site using standard precision mode of Glide docking protocol. Docking calculations were performed using Glide genetic algorithm. Interactions were characterized based on G score (most negative interaction energy).

Preparation of concanavalin A anchored polyethylene sebacate-nevirapine-gold nanoparticles

A solution of CON in PBS buffer was added to the PES-NVP-AuNPs dispersion to achieve a nanoparticles:CON ratio 1:0.5 and 1:1. The dispersion was incubated at 37^{o}C for 1 h and analyzed by spectrofluorimetry in the range of 300–500 nm maintaining the excitation wavelength at 280 nm[22]. The effect of time (15, 30, 45 & 60 min) on fluorimetric emission was evaluated against NVP and NVP free nanoparticles. Unloaded CON concentration was determined by comparing fluorescence intensity with standard CON at 335 nm. % CON binding was calculated using the following equation

$$\% \text{ CON binding} = \mathbf{(}[CON]_{total}\text{-}[CON]_{unloaded}\mathbf{)}/[CON]_{total} \times 100$$

Entrapment efficiency

Nananoparticulate dispersion was centrifuged at 20,000 rpm and 25ºC for 20 min and supernatant was analyzed by UV-1650 PC spectrophotometer (Shimadzu, Japan) at 283 nm for the determination of free NVP. The % EE was calculated using the following equation

$$\% \text{ EE} = NVP_{total}\text{-}NVP_{supernatant} / NVP_{total} \text{ X } 100$$

Particle Size and zeta potential analysis

Particle size and zeta potential of surface unmodified and modified nanoparticles were measured using ZetaSizer Nano ZS, (Malvern Instruments Ltd, Malvern UK) at 28^{o}C. Prior measurement nanoparticles were diluted with miliQ water in order to get a particle count in the range of 300-500.

Drug loading

Freeze dried PES-NVP-AuNPs (10 mg) were dissolved in methanol (5 mL), sonicated for 15 min, centrifuged at 20^{o}C , 14000 rpm for 15 min. Supernatant on suitable dilution with water was analyzed by UV spectrophotometer at 283 nm for NVP content. Percent Drug loading (DL %) was calculated using the equation:

DL (%) = $W_{DL}/W_{NP}\times100$

W_{DL} = weight of drug in nanoparticles, W_{NP} = weight of nanoparticles

UV spectroscopy

UV–visible absorption spectra of AuNPs and PES-NVP-AuNPs were recorded in the range of 200-600 nm on UV spectrophotometer, using miliQ water as a reference.

Fourier Transform Infrared Spectroscopy (FTIR)

FTIR spectra of NVP, PES, PES-NVP-AuNPs, CON and CON-PES-NVP-AuNPs were recorded on Shimadzu FTIR IRAffinity-1 Miracle 10 spectrophotometer. Samples were mulled with anhydrous potassium bromide (KBr) and further compressed to form a thin pellet using hydraulic press. FTIR analysis of prepared KBR pellet was recorded in the range 450-4000cm^{-1}.

Diffential Scanning Calorimetry (DSC)

Samples were weighed (5 mg) in aluminum pans, sealed, and were subjected to DSC analysis on Perkin Elmer Pyris 6 DSC thermal analysis instrument. The DSC thermograms were recorded by heating samples at a scan rate of 10°C/min from 40°C and 300°C in nitrogen atmosphere with empty sealed aluminum pan as a reference.

X Ray Diffractometry (XRD)

X-Ray diffraction (XRD) patterns of PES, CON and nanoparticles were recorded using Philips Pro Expert diffractometer (PANalytical B.V., Almelo, The Netherlands), equipped with nickel filtered Cu Kα radiation operated at 30 mA current and 40 kV voltage. XRD scans of all samples were measured in the range of 10°–60° (2θ).

Scanning Electron Microscopy (SEM)

A drop of nanoparticulate dispersion diluted in miliQ water was deposited on carbon tape adhered onto metal stub with double-sided adhesive tape and air dried. Morphology and energy dispersive X- ray analysis (EDAX) of nanoparticles was determined by SEM (Zeiss DSM 940A SEM; Oberkochen, Germany).

Transmission Electron Microscopy (TEM)

The morphological analysis of PES-NVP-AuNPs and CON-PES-NVP-AuNPs was performed using TEM (CM 200, Philips Briarcliff Manor, USA). A drop of diluted nanoparticulate dispersion was placed on carbon grids (Ted Pella, Inc, Redding, CA). The carbon grid was further subjected to staining by addition of drop of 2 % w/v uranyl acetate. The grid was air dried at 28^{o}C for 24 h and imaging was performed using TEM instrument.

Freeze-Drying

Freeze drying of nanoparticles was carried out on Labconco freeze dryer (FreeZone 4.5, USA) using trehalose as cryoprotectant at 1:2, 1:4, 1:10 by weight nanoparticles: trehalose ratio. Nanoparticles pellet obtained after centrifugation was dispersed in solutions containing different concentrations of trehalose. The samples were frozen at -70°C for 12 h and then subjected to freeze-drying for 36-48 h at a vacuum pressure of $10\text{-}50\times10^{-3}$ bar, with the condenser surface temperature maintained at less than -50°C.

Residual solvent analysis

To determine residual solvent in freeze dried nanoparticles, headspace gas chromatography was performed using Chemito GC 8610 GAS CHROMATOGRAM equipped with flame ionization detector. The gas chromatograph comprised BP capillary column having 30 m length and 0.3 mm internal diameter. GC injection port & detector were kept at 200^{o}C and 240^{o}C respectively. The flow of nitrogen gas was maintained at 1 mL/min. The oven temperature initially maintained at 60^{o}C for first 2 min and further temperature increased to 240^{o}C for another 5 min at rate of 10^{o}C min^{-1}. The standard consisted 10 ppm concentration of dichloromethane (DCM) in dimethyl sulphoxide (DMSO) was placed in headspace vial. The vial was sealed and residual solvent analysis was performed using abovementioned procedure. For the determination of residual solvent in nanoparticles, 100 mg nanoparticles were dissolved in 1 mL DMSO in headspace vial and analysis was performed.

***In vitro* drug release study**

Drug release studies of NVP from PES-NVP-AuNPs and CON-PES-NVP-AuNPs were performed by a dialysis bag method. Briefly, nanoparticles equivalent to 14 mg drug were filled in dialysis bag (MWCO: 12,000-14,000 Da, Himedia Laboratories Pvt. Ltd., Mumbai, India) and sealed. Dialysis bag was placed in basket of USP dissolution apparatus I (Electrolab, Mumbai, India) and dissolution (n=6) was performed at 100 rpm using 900 mL phosphate buffer pH 7.4 maintained at 37 ± 0.5ºC. At specified time points (0.5, 1, 2, 4, 6, 8, 12, 16, 20 and 24 h), 10 mL sample was withdrawn and replaced with fresh 10 mL medium. The amount of NVP released was determined using UV spectrophotometer at 283 nm. Percent cumulative drug release versus time profiles were plotted. *In-vitro* release data was fitted to kinetic models such as zero-order, first-order, Higuchi equation, Korsemeyer–Peppas equation and Hixson–Crowell equation[23, 24].

Stability study

Nanoparticles were evaluated for stability as per ICH guidelines. Nanoparticles placed in glass vials were kept at 30°C/65 % RH and 40°C /75 % RH. At the end of 3, 6, 12 months samples were evaluated for changes in particle size, drug content. Drug content was determined by HPLC using

a procedure described earlier in section 2.7. The HPLC Jasco LC900 system consisted of Jasco PU-980 Intelligent HPLC pump, Jasco UV-975 Intelligent UV/VIS detector coupled with a Rheodyne injector, 00 µL sample loop and Borwin Chromatography Software (Version 1.50) integrator software. Analysis was performed on Spherisorb® C18 column (5 µm, 4.6 mm × 250 mm, Waters, USA) at wavelength 212 nm using 50 mM sodium dihydrogen orthophosphate: acetonitrile (75:25) mobile phase at 1mL/min flow rate.

Statistical analysis

All experimental data values are presented as mean ± standard deviation (SD). Results were statistically analyzed using student's t-test or one-way ANOVA Dunnet post test using GraphPad Prism 5 (La Jolla, CA 92037 USA). P value < 0.05 was considered to be statistically significant

RESULTS AND DISCUSSION

Macrophages provide a safe haven for the HIV and are responsible for dissemination of the infection various tissues[8, 25]. Nevirapine an important drug in the HAART is known to cause fatal hepatotoxicity. Targeted delivery of antiretrovirals to the macrophages has shown great promise in treating infections. Folate-modified atazanavir/ritonavir developed for macrophage targeting enhanced macrophage uptake, retention, antiretroviral activities and demonstrated five-fold enhanced plasma and tissue drug levels in mice[26]. Nowacek designed nanoparticles of a combination of ritonavir, indinavir and efavirenz for macrophage targeting and revealed rapid uptake of the nanoparticles in < 30 min, sustained release over 14 days in macropahges and promising reduction in progeny virion production & HIV-1 p24 antigen[27]. Therefore macrophage targeted nevirapine delivery represents promising approach for improving its efficacy and safety. Further it is postulated that controlling the rate of the drug release from the delivery system could prolong duration of action, decrease adverse effects and hence improve patient compliance.

Preparation of polyethylene sebacate-nevirapine-gold nanoparticles by double emulsion solvent evaporation (DESE)

A double emulsion solvent evaporation (DESE) method of nanoparticles preparation is exploited for loading drugs onto preformed gold nanoparticles[28]. DESE has also been reported for the preparation of nanoparticles in microparticles[29]. Hence in the present study the DESE method was successfully manipulated to prepare core shell nanoparticles comprising AuNPs as the core and NVP loaded PES as the shell of the nanoparticles. The positive shift in the surface plasmon resonance from 526 to 564 nm confirmed the presence of a shell around the AuNPs, while in the UV spectrum a peak at 283 nm, a characteristic for aromatic amine transitions of NVP, indicated

incorporation of NVP in the nanoparticles (Figure1a). The increase in particle size (242.9 ± 17.52 nm) and decrease in zeta potential zeta potential of (-26.7 ± 1.67 mV) of PES-NVP-AuNPs compared to AuNPs (71.3 ± 4.5 nm particle size and -18 ± 1.9 mV zeta potential) further substantiated core shell formation. Entrapment efficiency of > 75 % was observed at all AOT concentrations (Figure 1b). A significant decrease in particle size ($p < 0.001$) from greater than 2000 nm to around 250 nm was observed with increase on AOT concentration from 0.15 to 0.25 w/v. AOT promotes hydrodynamic stabilization above its critical micelle concentration (0.24% w/v) by adsorbing at droplet interface, thereby enabling smaller droplet formation[30].

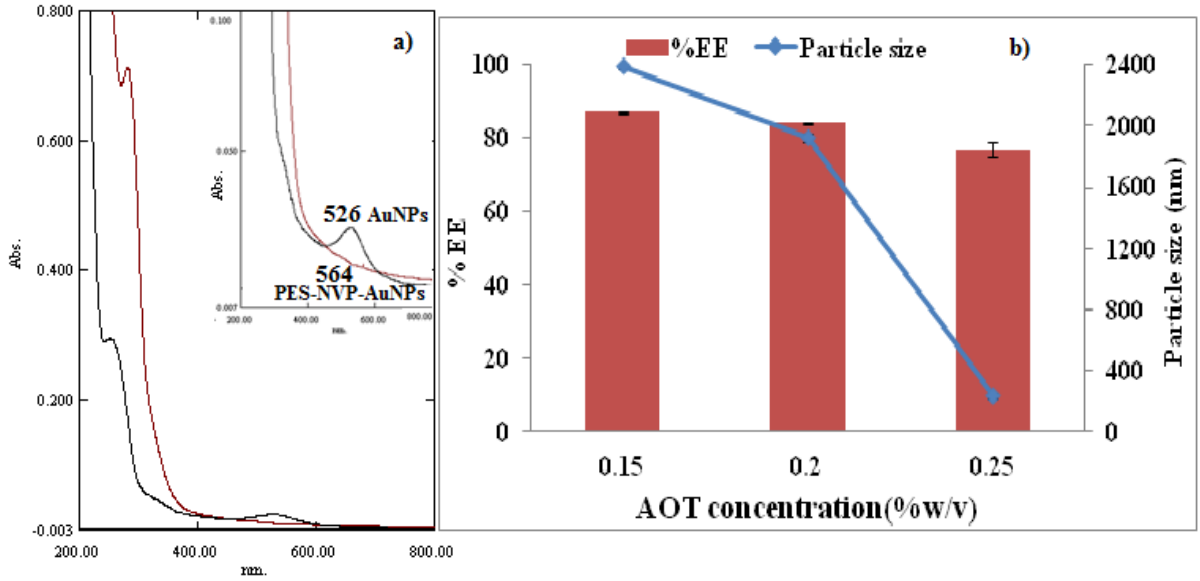

Figure 1: UV spectrum of AuNPs (black curve) and PES-NVP-AuNPs (brown curve) (a), Effect of AOT concentration on particle size and entrapment efficiency (b)

Molecular docking study of concanavalin with nevirapine and polyethylene sebacate

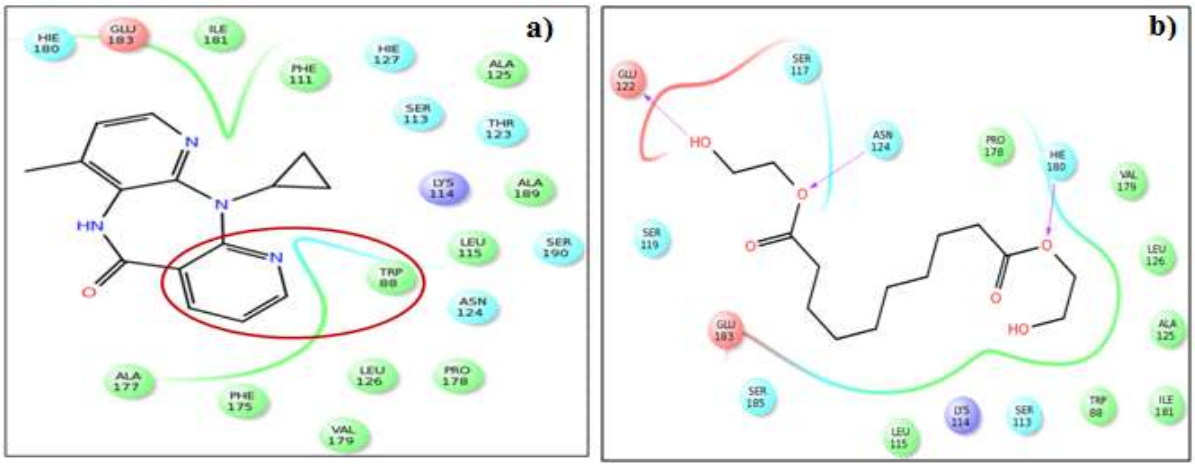

Figure 2: 2-D representation of NVP (a) and PES oligomer (b) docking with CON

Molecular docking a well established computational technique was used to predict interactions of CON with NVP and PES oligomer. Sitemap analysis of CON yielded 4 binding sites; amongst these sites site I and site III were found to be present near mannose binding site and demonstrated low sitescore, while site II and IV exhibited site score of 0.676 and 0.623 respectively. Based on the sitescore, site II and IV were chosen for docking studies. Site IV revealed poor ligand docking, while the results of docking with site II are demonstrated in Figure 2. TRP 88 & PHE 175 residues of the CON were found to strongly interact with NVP (Figure 2a), suggesting the role of hydrophobic interactions of CON with NVP. This was confirmed by the high glide g score of -5.25 kcal/mol, glide energy of -27.25 kcal/mol and glide emodel score of -35.28 kcal/mol. PES formed hydrogen bonds with GLU122, ASN 124 and HIE 180 as demonstrated in Figure 2b, and exhibited glide g score of -1.26, glide energy of -39.44 kcal/mol and glide emodel score of -37.77 kcal/mol. Thus the more negative G score of NVP confirmed stronger affinity of NVP with CON.

Preparation of concanavalin anchored polyethylene sebacate-nevirapine-gold nanoparticles

Targeting ligand can be loaded onto the nanoparticles via covalent or non-covalent i.e physical adsorption methods. Although covalent interaction provides stronger attachment covalent method has several limitations like difficult to synthesize, laborious, expensive and also chemical modification may lead to inactivation of biomolecule, reduced efficiency of drug release or incomplete intracellular processing the conjugate[31]. In contrast non-covalent (physical adsorption) is a more practical and efficient approach for loading targeting ligand. It allows incorporation of targeting ligand in their original form thus avoiding intracellular processing issues associated with the covalent approach. Hence, in the present study physical adsorption was exploited for loading mannose receptor ligand concanavalin on the surface of PES-NVP-AuNPs. CON was successfully loaded on the surface of PES-NVP-AuNPs by simple incubation. Spectrofluorimetric evaluations confirmed anchoring of CON onto the PES-NVP-AuNPs (Figure 3a & b). The tryptophan residues (TRP at 40, 88, 109 & 182) present in the CON monomer are responsible for its fluorescence[22]. Binding of substrate with CON through hydrophobic interactions results in reduction in trptophan fluorescence. A high and maximum binding of > 80 % was observed at nanoparticles: CON ratio 1:0.5 (Figure 3a). Further increase in CON concentration revealed no enhancement in binding (Figure 3b). Incubation of nanoparticles with CON (1:0.5) for 60 min revealed comparable fluorescence quenching with > 80% binding at 15 min and above suggesting 15 min as an adequate time for reaction (Figure 3c). Blank PES-AuNPs incubated with CON revealed no fluorescence quenching (Figure 4a), however decreased CON fluorescence intensity was evident on incubation of CON with NVP, thus confirmed the strong binding of NVP with CON (Figure 4b). Anchoring

of CON to the nanoparticles could be attributed to hydrophobic interactions between the aromatic residues of NVP and the TRP residues of CON.

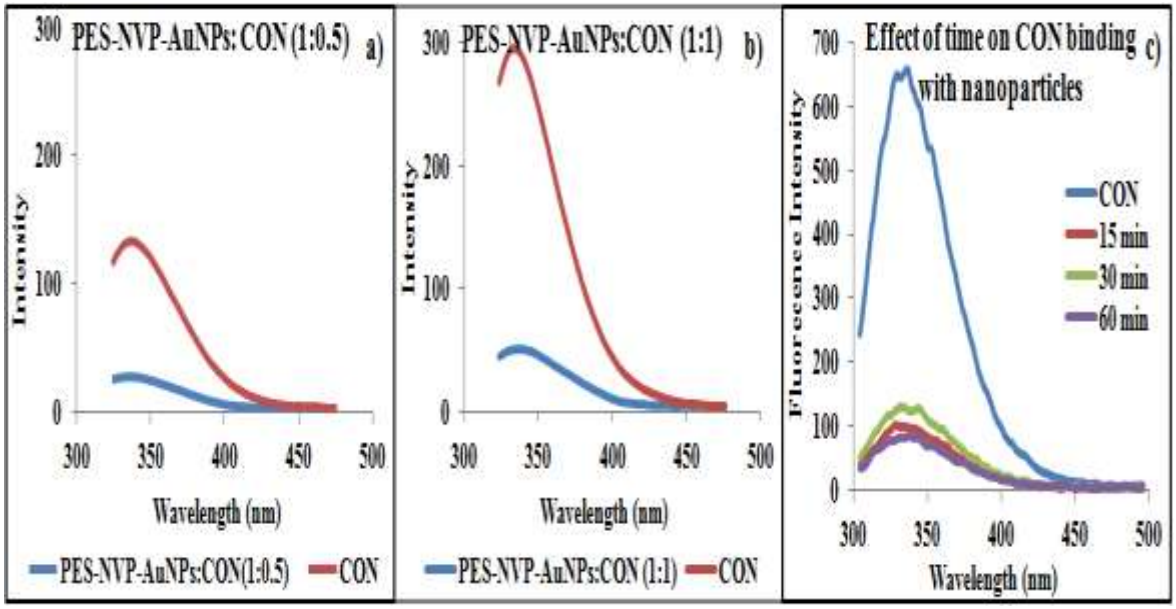

Figure 3: Fluorescence quenching of CON on interaction with nanoparticles at 1:0.5 (a), 1:1 (b) nanoparticles: CON concentration and Effect of time of nanoparticles & CON incubation on CON fluorescence (c)

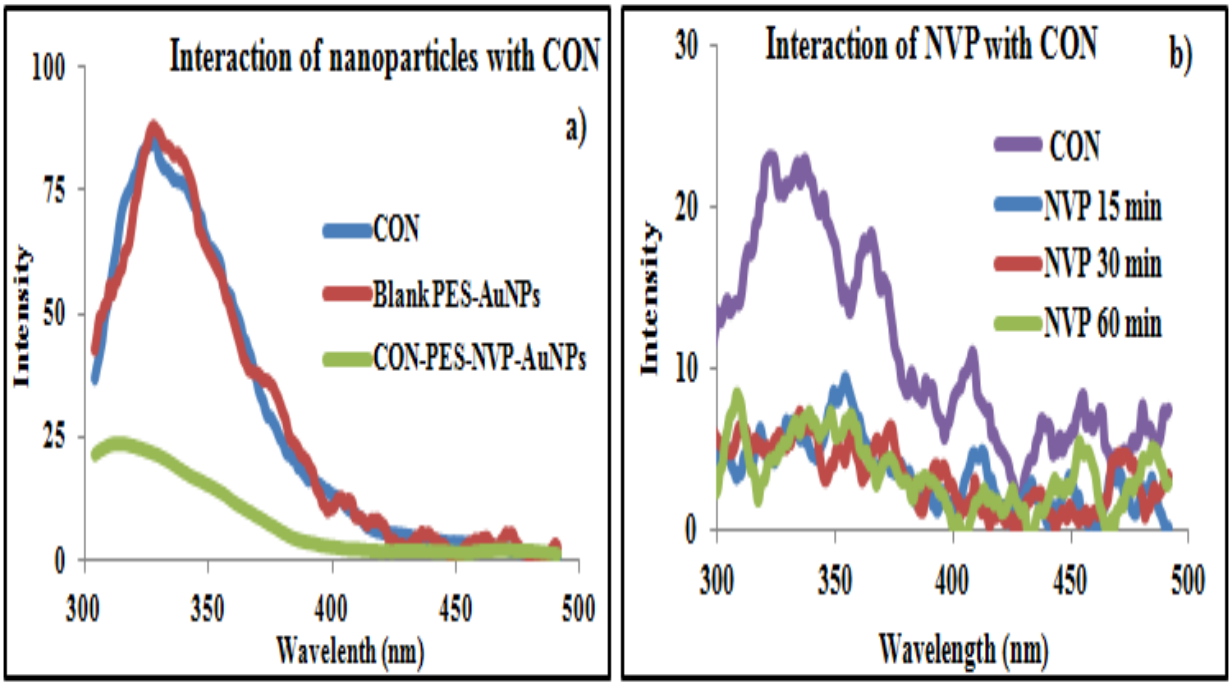

Figure 4: Fluorescence quenching of CON upon interaction with nanoparticles (a) and NVP (b).

The particle size and zeta potential of CON-PES-NVP-AuNPs was found to be to 259.3 ± 14.56 and -11.1 ± 0.56 mV respectively. The change in zeta potential of the nanoparticles on CON

loading further confirmed its efficient loading. Therefore physical adsorption or non-covalent method presents an easy and simple approach for loading of targeting ligand onto nanoparticles.

FTIR analysis

Further, interactions of components present in the nanoparticles were also evaluated by FTIR. Plain NVP revealed N-H and C=O stretching at 3188 and 1642 cm^{-1} respectively, while PES demonstrated a peak for –OH at 3462 cm^{-1} (Figure 5). PES-NVP-AuNPs exhibited a positive shift for NVP stretching at 3197 cm^{-1} with an additional broad peak at 3456 cm^{-1}, whereas CON-PES-NVP-AuNPs revealed absence of the NH stretching peak at 3188 and a broad peak from 3500-3200 cm^{-1}, indicating hydrogen bonding between the components.

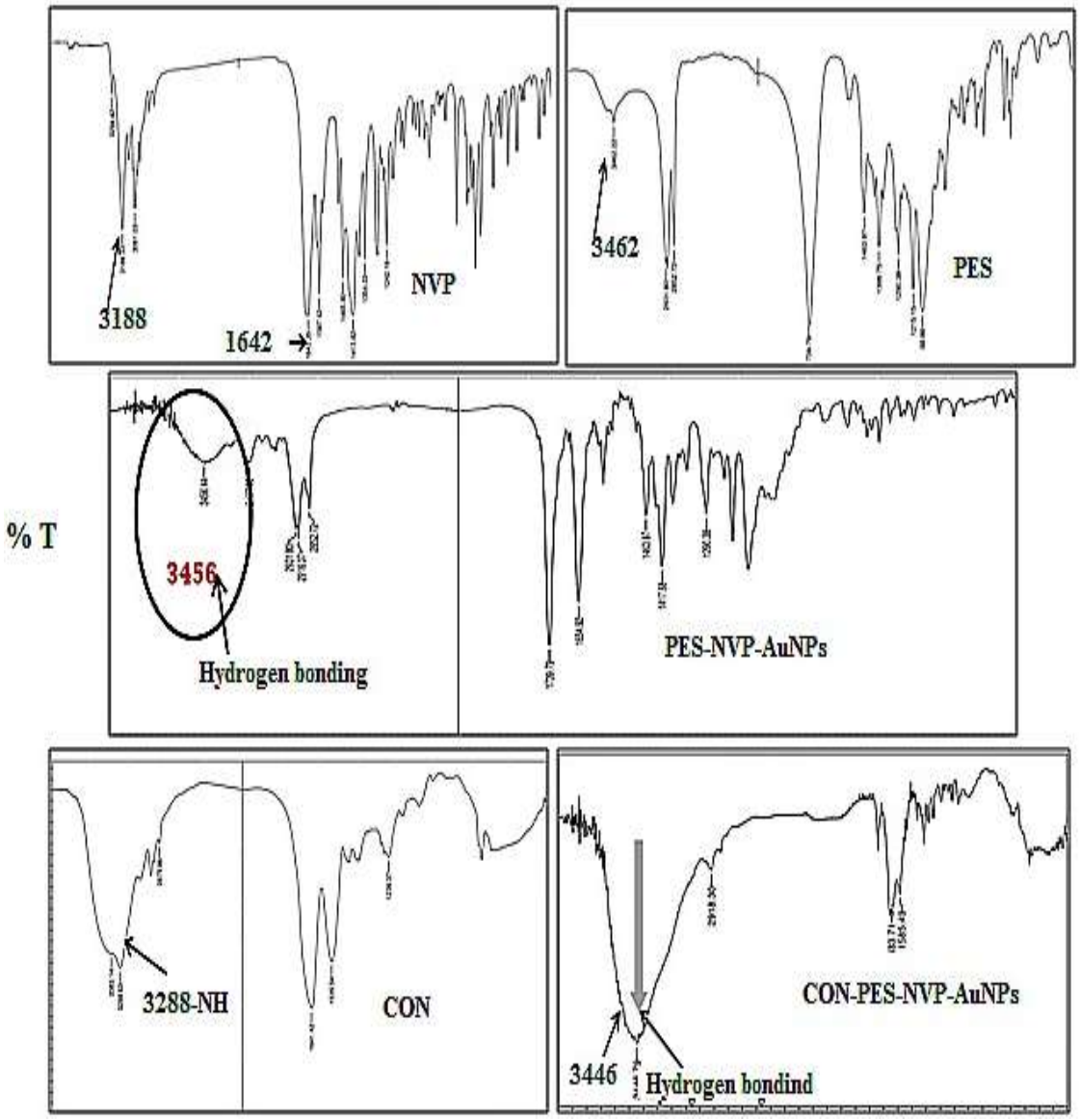

Figure 5: FTIR spectrum of NVP, PES, PES-NVP-AuNPs, CON and CON-PES-NVP-AuNPs

Freeze drying of nanoparticles

The physicochemical properties influence efficiency of the delivery system [32]. Nanodispersions if stored as a suspension agglomeration, drug leakage and drug degradation may occur. Freeze drying/lyophilization ensure the long term conservation, improve physical stability and increase the shelf life of polymeric nanoparticles[33-35]. Moreover, redispersibility of nanoparticles is crucial parameter which otherwise results in loss of their special properties. Trehalose was selected as cryoprotectant in present study because of its well established best cryoprotection properties. Trehalose offer advantages like: less hygroscopicity, higher glass transition temperature and enables formation of hydrogen bond with nanoparticles[36]. Nanoparticles: trehalose ratio of 1:10 exhibited desired cryoprotection (Sf/Si ratio < 1.3) while, significant enhancement in particle size was observed at lower trehalose concentration.

DSC and XRD analysis

The disappearance of the NVP melting endothermic in DSC thermogram (Figure 6a) and significant reduction in intensity of sharp diffraction peaks in the XRD pattern (Figure 6b) exhibited by nanoparticles with and without CON suggested reduced crystallinity or amorphization of both NVP and PES in the nanoparticles.

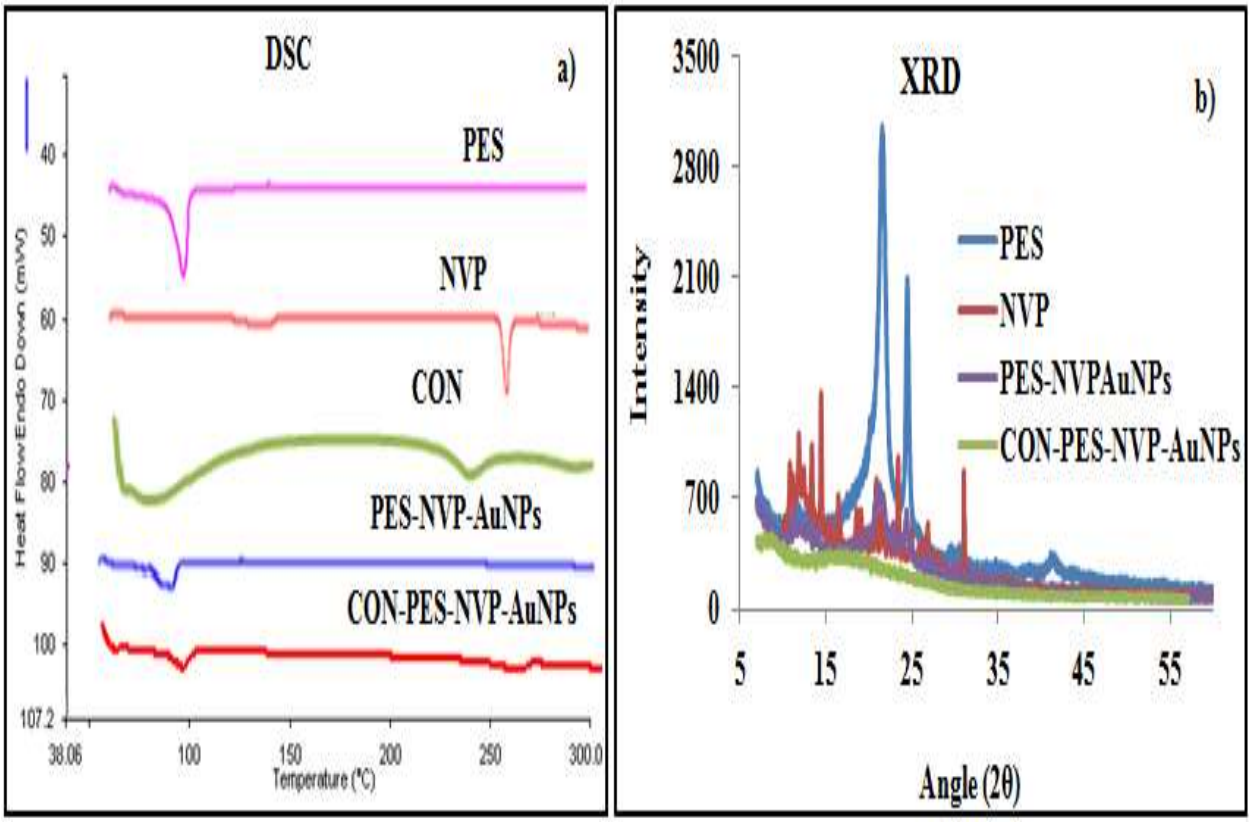

Figure 6: DSC thermograms (a) and XRD patterns (b) of NVP, PES, CON, PES-NVP-AuNPs, CON and CON-PES-NVP-AuNPs

SEM and TEM analysis

SEM revealed formation of spherical particles having smooth surfaces (Figure 7a and d). The characteristic optical absorption peaks of gold nanocrystallites observed in the SEM-EDAX spectra of PES-NVP-AuNPs and CON-PES-NVP-AuNPs (Figure 7b and e) confirmed the presence of gold in the nanoparticles. While the TEM micrographs of PES-NVP-AuNPs and CON-PES-NVP-AuNPs substantiated formation of core shell nanoparticles with spherical shape (Figure 7 c & f). The results of TEM analysis suggested particle size of the both the nanoparticles in the range of 200-300 nm which was in good agreement with dynamic light scattering results.

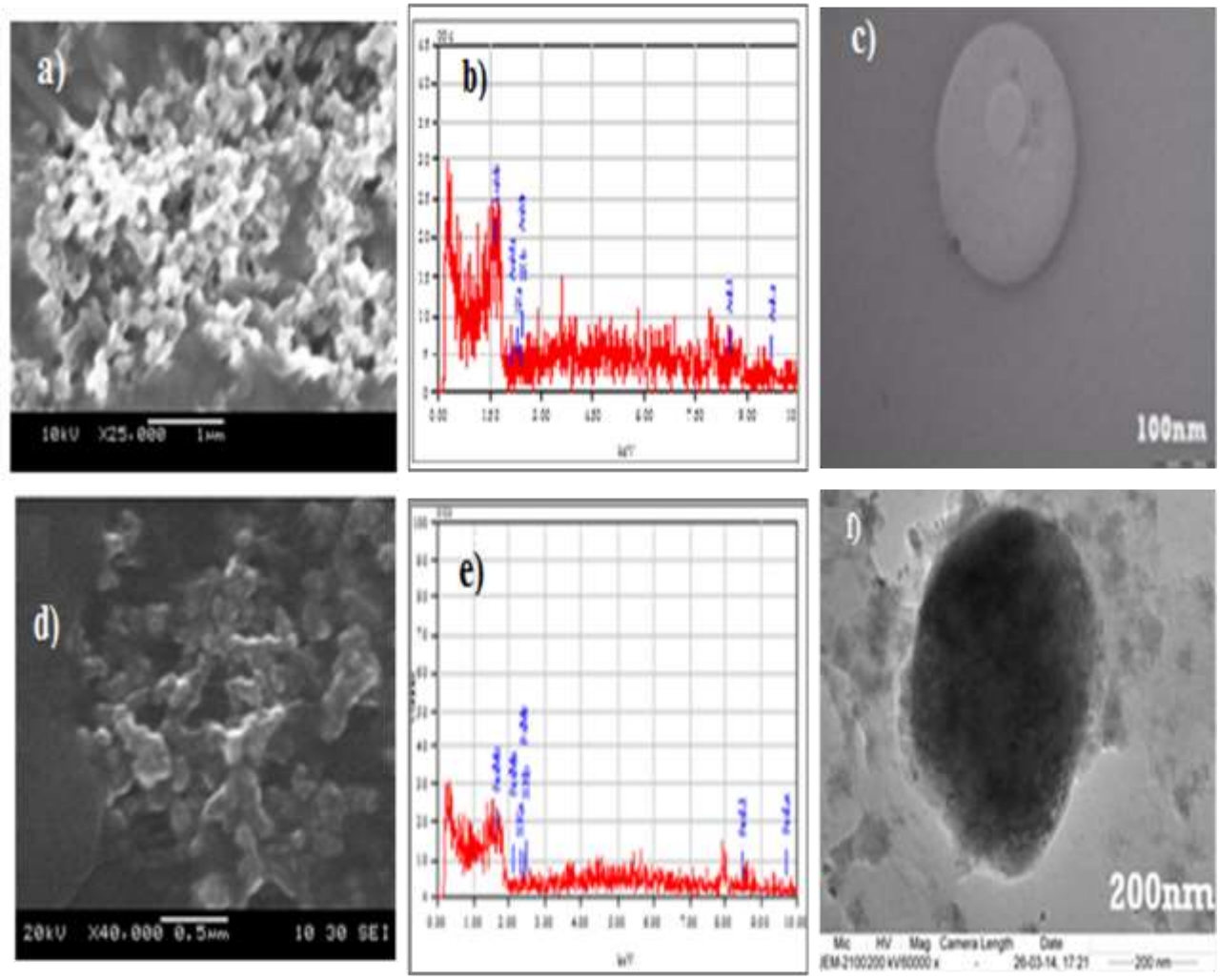

Figure 7: SEM image (a), EDAX pattern (b) and TEM image (c) of PES-NVP-AuNPs, SEM image (d), EDAX pattern (e) and TEM image (f) of CON-PES-NVP-AuNPs

Residual solvent analysis

GC analysis revealed no detectable amount of DCM (LOD 5 ppm) thereby complying with the ICH standards of < 600 ppm[37]. Low viscosity (0.413 cps at 25^{o}C) and low boiling point (39.6^{o} C) of DCM offered faster removal.

***In-vitro* drug release study**

The % cumulative NVP release in 24 h from PES-NVP-AuNPs and CON-PES-NVP-AuNPs was 35.83 ± 0.89 and 33.59 ± 1.3 % respectively (Figure 8). The dissolution profile of CON-PES-NVP-AuNPs was found to be similar with PES-NVP-AuNPs suggesting CON anchoring did not influence NVP release. To investigate dissolution kinetics and drug release mechanism different kinetics models, zero order, first order, Higuchi, Korsmeyer-Peppas and Hixon-Crowell were employed. The results of curve fitting models as depicted in table 1 revealed that in-vitro dissolution data from both the nanoparticles exhibited good correlation with Higuchian kinetics wherein drug release is found to be diffusion controlled[38].

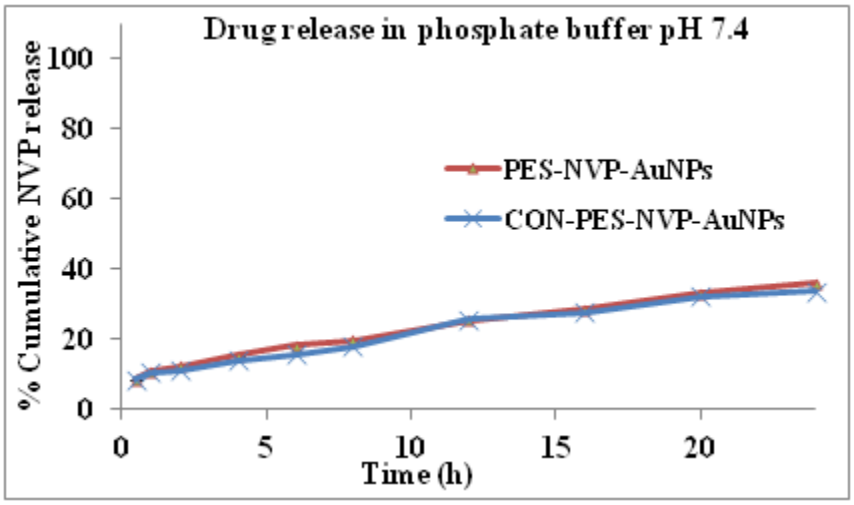

Figure 8: *In-vitro* NVP release profile from nanoparticles with and without CON in phosphate buffer pH 7.4

Table 1: Results of kinetic model fitting for NVP release from PES-NVP-AuNPs, CON and CON-PES-NVP-AuNPs

Model	**PES-NVP-AuNPs**			**CON-PES-NVP-AuNPs**		
	r^2	Slope	Intercept	r^2	Slope	Intercept
Zero order	0.985	1.143	9.972	0.9784	1.1138	9.1774
First order	0.953	-0.007	1.965	0.9504	-0.0067	1.9681
Higuchi	**0.988**	6.785	1.987	**0.9789**	6.5389	1.6206
Korsmeyer-Peppas	0.976	0.3734	0.998	0.9756	0.3734	0.9989
Hixon-Crowell	0.968	13.02	-3.901	0.9565	11.697	-2.2525

Stability study

Freeze dried PES-NVP-AuNPs and CON-PES-NVP-AuNPs were stable for 12 months at 30°C/60% RH and for 6 months at 40°C/75% RH. Both the nanoparticles exhibited good stability

as per ICH guidelines with respect to drug content > 90 %, good redispersibility in water, no significant change in particle size (Sf/Si ratio < 1.3).

CONCLUSION

We present the simple physical adsorption technique for the design of targeted delivery system for nevirapine. Sustained drug release and high stability remains other positive attributes of the system.

ACKNOWLEDGMENT

Authors are indebted to University Grants Commission, Government of India for providing research financial assistance.

REFERENCES

1. Saksena NK, Wang B, Zhou L, Soedjono M, Ho YS, Conceicao V. HIV reservoirs in vivo and new strategies for possible eradication of HIV from the reservoir sites. HIV/AIDS – Research and Palliative Care 2010: 2; 103-122.
2. Garg M, Asthana A, Agashe HB, Agrawal GP, Jain NK. Stavudine-loaded mannosylated liposomes: in-vitro anti-HIV-I activity, tissue distribution and pharmacokinetics. J Pharm Pharmacol 2006: 58; 605–616.
3. Raimar L, Jorg K. Macrophage targeting of azidothymidine: a promising strategy for AIDS therapy. AIDS research and human retroviruses 1996: 12; 1709-1715.
4. Roy S, Wainberg MA. Role of the mononuclear phagocyte system in the development of acquired immunodeficiency syndrome (AIDS). J Leuk Biol. 1988: 43; 91-97.
5. Meltzer MS, Skillman DR, Hoover DL, Hanson BD, Turpin JA, Kalter DC, Gendelman HE. Macrophages and the human immunodeficiency virus. Immunol Today 1990: 6; 217-223.
6. Ramana LN, Sethuraman S, Ranga UR, Krishnan UM. Research development of a liposomal nanodelivery system for nevirapine. Journal of biomedical science 2010: 17; 57.
7. Van Vlerken LE, Amiji MM. Multi-functional polymeric nanoparticles for tumour-targeted drug delivery. Expert Opinion on Drug Delivery 200: 3; 205-216.
8. Ahsan F, Rivas IP, Khan MA, Torres Suarez AI. Targeting to macrophages: role of physicochemical properties of particulate carriers-liposomes and microspheres-on the phagocytosis by macrophages. J Controlled Release 2002: 79; 29–40.
9. Gagne¨ JF, De¨sormeaux A, Perron S, Tremblay MJ, Bergeron MG. Targeted delivery of indinavir to HIV-1 primary reservoirs with immunoliposomes. Biochimica et biophysica acta 2002: 1558; 198-210.

10. Kaur CD, Nahar M, Jain NK. Lymphatic targeting of zidovudine using surface- engineered liposomes. J Drug Target. 2008: 16; 798-805.
11. Jain SK, Gupta Y, Jain A, Saxena AR, Khare P, Jain A. Mannosylated gelatin nanoparticles bearing an anti-HIV drug didanosine for site specific delivery. Nanomedicine 2008: 4; 41-8.
12. Kaur A, Jain S, Tiwary AK. Mannan-coated gelatin nanoparticles for sustained and targeted delivery of didanosine : in vitro and in vivo evaluation. Acta. Pharm. 2008: 58; 61-74.
13. Dutta T, Jain NK. Targeting potential and anti-HIV activity of lamivudine loaded mannosylated poly (propyleneimine) dendrimer, Biochimica et Biophysica Acta 2007: 1770; 681– 686.
14. Dutta T, Agashe HB, Garg M, Balakrishnan P, Kabra M, Jain NK. Poly (propyleneimine) dendrimer based nanocontainers for targeting of efavirenz to human monocytes/macrophages in vitro. Drug target. 2007: 15; 89-98.
15. Dutta T, Garg M, Jain NK. Targeting of efavirenz loaded tuftsin conjugated poly (propyleneimine) dendrimers to HIV infected macrophages in vitro. Eur J Pharm Sci. 2008: 34; 181-9.
16. Muller CD, Schuber F. Neo-mannosylated liposomes: synthesis and interaction with mouse kupffer cells and resident peritoneal macrophages. Biochim. Biophys. Acta Ser. Biomembr. 1989: 986; 97–105.
17. Yachi K, Kikuchi H, Yamauchi H, Hirota S, Tomikawa M. Distribution of liposomes containing mannobiose esters of fatty acid in rats. J. Microencaps. 1995: 12, 377–388.
18. Sharma A, Sharma S, Khuller GK. Lectin-functionalized poly (lactide-co-glycolide) nanoparticles as oral/aerosolized antitubercular drug carriers for treatment of tuberculosis. J. Antimicrob. Chemother. 2004: 54; 761–766.
19. Banerjee T, Nand Kishore. Binding of 8-Anilinonaphthalene sulfonate to dimeric and tetrameric concanavalin A: energetics and its implications on saccharide binding studied by isothermal titration calorimetry and spectroscopy. J. Phys. Chem. B. 2006: 110; 7022-7028.
20. Pashov A, MacLeod S, Saha R, Perry M, VanCott TC, Emmons TK. Concanavalin A binding to HIV envelope protein is less sensitive to mutations in glycosylation sites than monoclonal antibody 2G12. Glycobiology 2005: 15; 994–1001.
21. More AB, Chilgunde SN, Kamble JC, Patil PS, Malshe VC, Vanage GR, Devarajan PV. Polyethylene sebacate: genotoxicity, mutagenicity evaluation and application in periodontal drug delivery system. J Pharm Sci. 2009: 98; 4781-4795.

22. Rao MVR, Atreyi M, Rajeswari MR. Fluorescence studies on concanavalin A. Biosci 1984: 6; 823–828.
23. Shivakumar HN, Patel PP, Desai BG, Ashok P, Arulmozhi S. Design and statistical optimization of glipizide loaded lipospheres using response surface methodology. Acta Pharm. 2007: 57; 269–285.
24. Shoaib MH, Tazeen J, Merchant HA, Yousuf RI. Evaluation of drug release kinetics from ibuprofen matrix tablets using HPMC. Pak J. Pharm. Sci. 2006: 19; 119-124.
25. Eisele E, Siliciano RF. Redefining the viral reservoirs that prevent HIV-1 eradication. Immunity 2012: 37; 377-388.
26. Puligujja P, McMillan J, Kendrick L, Li T, Balkundi S, Smith N, Veerubhotla RS, Edagwa BJ, Kabanov AV, Bronich T, Gendelman HE, Liu XM. Macrophage folate receptor-targeted antiretroviral therapy facilitates drug entry, retention, antiretroviral activities and biodistribution for reduction of human immunodeficiency virus infections. Nanomedicine 2013: 9; 1263-1273.
27. Nowacek AS, Miller RL, McMillan J, Kanmogne G, Kanmogne M, Mosley RL, Ma Z, Graham S, Chaubal M, Werling J, Rabinow B, Dou H, Gendelman HE. NanoART synthesis, characterization, uptake, release and toxicology for human monocyte-macrophage drug delivery. Nanomedicine 2009: 4; 903-917.
28. Claudia W, Eric D. Influence of the microencapsulation method and peptide loading on poly(lactic acid) and poly(lactic-co-glycolic acid) degradation during in vitro testing. J Controlled Release 1998: 51; 327–341.
29. Lee YS, Johnson PJ, Robbins PT, Bridson RH. Production of nanoparticles-in-microparticles by a double emulsion method: A comprehensive study. European J Pharma Biopharma 2013: 83; 168–173.
30. Moulik SP, Mukherjee K. On the versatile surfactant aerosol-OT (AOT): its physicochemical and surface chemical behaviors and uses. Proc. Indian Natn Sci Acad. 1996: 62; 215-232.
31. Bhattacharya R, Patra CR, Earl A, Wang S, Katarya A, Lu L, Kizhakkedathu JN, Yaszemski MJ, Greipp PR, Mukhopadhyay D, Mukherjee P. Attaching folic acid on gold nanoparticles using noncovalent interaction via different polyethylene glycol backbones and targeting of cancer cells. Nanomed. Nanotechnol. Biol. Med. 2007: 3; 224–238.
32. Bozdag S, Dillen K, Vandervoort J, Ludwig A. The effect of freeze-drying with different cryoprotectants and gamma-irradiation sterilization on the characteristics of ciprofloxacin HCl-loaded poly(D,L-lactide-glycolide) nanoparticles. J. Pharm Pharmacol. 2005: 57; 699–707.

33. Roy D, Guillon X, Lescure F, Couvreur P, Bru P, Breton P. On shelf stability of freeze-dried poly(methylidene) malonate, nanoparticles. Int. J. Pharm. 1997: 148; 165-175.
34. Abdelwahed W, Degobert G, Fessi H. A pilot study of freeze drying of poly(epsiloncaprolactone) nanocapsules stabilized by poly(vinyl alcohol): formulation and process optimization. Int. J Pharm. 2006: 17; 178–188.
35. Kuleshova LL, MacFarlane DR, Trounson AO, Shaw JM. Sugars exert a major influence on the vitrification properties of ethylene glycol-based solutions and have low toxicity to embryos and oocytes. Cryobiology 1999: 38; 119–130.
36. De Jaeghere F, Alle´mann E, Feijen J, Kissel T, Doelker E, Gunny R. Freeze-drying and lyopreservation of diblock and triblock poly(lactic acid)–poly(ethylene oxide) (PLA–PEO) copolymer nanoparticles. Pharm. Dev. Tech. 2000: 5; 473-483.
37. Han EJ, Chaung AH, Oh IJ. Analysis of residual solvents in poly(lactide-co-glycolide) nanoparticles. Journal of pharmaceutical investigation, 2012: 42; 251–256.
38. Khuroo T, Verma D, Talegaonkar S, Padhi S, Panda AK, Iqbal Z. Topotecan–tamoxifen duple PLGA polymeric nanoparticles: Investigation of in vitro, in vivo and cellular uptake potential, Int J Pharma 2014: 473; 384–394.